# Tailoring Mechanical and Thermal Properties of PVDF by Incorporating [BMIM][$BF_4$] via Solution Casting Technique

Kavita Rani[1], Anurekha Sharma[1,*] and Yashashchandra dwivedi[2]

[1]*Department of Electronic Science, Kurukshetra University, Kurukshetra, Haryana, India, 136118*

[2]*Department of Physics, National Institute of Technology, Kurukshetra, Haryana, India, 136119*

**Abstract:** This study focuses on the synthesis of Ionic liquid (IL) based Poly(vinylidene fluoride) (PVDF) films using the solution casting method. In this work 1-butyl-3-methylimidazolium tetrafluoroborate ([BMIM][$BF_4$]) IL was used. The main aim of this work is to understand how the addition of 1-butyl-3-methylimidazolium tetrafluoroborate ([BMIM][$BF_4$]) IL, affects the structural, mechanical, and thermal properties of PVDF films. Different IL concentrations ranging from 3wt.% to 15wt.% were added to PVDF, and the prepared films were analyzed using various characterization techniques. The results show that the addition of IL enhances the β-phase of PVDF, which is important for sensors, actuators, and energy harvesting applications. The 86.6% β-phase content was observed at 12 wt.% IL in PVDF. This β-phase content is found to be highest as compared to that reported in the literature of PVDF/ ([BMIM][$BF_4$]) film prepared by solution casting method. Structural studies using XRD and FTIR confirmed the phase transformation. Surface morphology analysis SEM revealed that the IL was well dispersed within the PVDF matrix, leading to uniform and improved film structure. Mechanical testing showed that tensile strength increased by 47.85% and elongation at break increased by 203.1% with addition of 12 wt.% IL. This improvement is also found to be highest as compared to that reported in the literature. The thermal analysis shows a decrease in thermal stability with the incorporation of IL. However, the solution cast films remained stable up to around 327 °C, and leaving a residue ~ 36.2% at 700 °C. These improved properties make PVDF/[BMIM][$BF_4$] films promising candidates for use in sensors, actuators, and energy harvesting or storage devices.

**Keyword –** PVDF, $BMIMBF_4$, Solution casting, Mechanical strength, Thermal stability.

## 1. INTRODUCTION

Poly(vinylidene fluoride) (PVDF) gains the most attention due to its combination of flexibility, biocompatibility, chemical stability, thermal stability and electroactive properties [1]. PVDF is a semi-crystalline polymer whose electroactive behavior originates from the orientation of molecular dipoles into its crystal structure. The polymer can exist in several crystalline phases namely α, β, γ, and δ. Each of these phases exhibit distinct chain conformations and dipole arrangements[2, 3]. The α-phase is nonpolar and piezoelectrically inactive. The β-phase exhibits an all-trans (TTTT) chain conformation, which aligns all dipoles in the same direction, therefore leading to a high net polarization and strong piezoelectric and ferroelectric behavior [4-6], hence is desirable for sensors, actuators, capacitor and energy harvesting applications. The γ-phase, with a T3GT3G′ conformation, possesses partial polarity and therefore exhibits intermediate electroactive properties between α and β phases [7, 8]. The ability to control the formation and alignment of these crystalline phases is a key to tuning the piezoelectric performance of PVDF. Several approaches have been used to transform the α to β phase in PVDF including mechanical stretching [9], filler addition such as incorporation ceramic and ionic liquids [10], electrospinning [11], heat annealing [12], high electric field poling [13], or solution processing under specific conditions [5]. Among these approaches, the incorporation of ionic liquids (ILs) has emerged as a promising and efficient strategy due to their unique physicochemical properties such as high ionic conductivity, low volatility, good thermal stability, and strong interaction capability with polymer chains. ILs such as 1-octadecyl-3-methylimidazolium bromide ([OMD]Br) [14], 1-ethyl-3-methylimidazolium tetrafluoroborate ([Emim][$BF_4$]) [15], 1-ethyl-3-methylimidazolium tetrafluoroborate ([C2mim][BF4]) [16], 1-butyl-3-methylimidazolium hexafluorophosphate ([BMIM][$PF_6$]) [17], and 1-butyl-3-methylimidazolium tetrafluoroborate ([BMIM][$BF_4$])[18] have been investigated to modify the properties of PVDF. These ILs can interact with PVDF chains through electrostatic interactions and ion–dipole forces, thereby influencing crystallization behavior and enhancing the formation of the electroactive β-phase. Among the various ionic liquids, [BMIM][$BF_4$] has gained attention in PVDF-based systems due to its physicochemical properties, such as high polarity, thermal stability, and strong compatibility with PVDF. The imidazolium cation present in [BMIM][$BF_4$] carries a $[BMIM]^+$ positive charge, which interacts with the electronegative $CF_2$– groups of PVDF. These electrostatic interactions result in the rotation of PVDF molecular chains and promote the transformation of the α-phase into β-phase. As a result, several studies have reported a increase in β-phase in PVDF/[BMIM][$BF_4$] composites by different fabrication methods such as solution casting, 3D

*Address correspondence to this author at the Department of Electronic Science, Kurukshetra University, Kurukshetra, Haryana, India, 136118;
E-mail: anurekhasharma@kuk.ac.in

Received on 05-10-2026 Accepted on 18-11-2026 Published on 23-11-2026

E-ISSN: 2410-4701/26

printing, N-TIPS and foaming machine techniques [18-21].

In addition to enhancing the β-phase of PVDF, its flexibility and thermal stability is also important factor for sensors, actuators and energy harvesting/ storage applications. Several experiments showed that ILs act as plasticizers in the PVDF matrix, helping to improve its flexibility and overall performance of PVDF composites[22]. As a result, these composites exhibit excellent ductility, optical transparency, ionic conductivity, and dielectric properties [22-26]. At the same time, some studies report that the incorporation ILs reduces the thermal stability of PVDF. However, the composite still maintains good thermal stability up to around 300 °C, which makes it suitable for applications in piezoelectric sensors, actuators, and energy storage/harvesting devices [27-29]. Several researchers have been reported that PVDF/[BMIM][$BF_4$] also acts as a plasticizers which improving the flexibility of PVDF. Ting he [20] reported that improve in flexibity of PVDF/[BMIM][$BF_4$] by 134.9% by using N-TIPS method but has not been reported the thermal stability. Y. Zhao [18] demonstrated that PVDF/[BMIM][$BF_4$] increases flexibility of PVDF upto 20% by using foaming techniques and has also not reported the thermal stability of the material. Shalu et. al [28] reported the [BMIM][$BF_4$] maintain the thermal stability of PVDF-HFP upto 320°C by solution casting but the mechanical properties were missing. Dzulkipli et.al [30] demonstrated the PVDF-HFP/[BMIM][$BF_4$] films which were thermally stable upto 300°C by solution casting. Similarly, Yongquan [31] prepared the PVDF-HFP/[BMIM][$BF_4$] film by solution casting which was thermally stable upto 370°C. However, most of the previous studies have focused on PVDF-HFP/[BMIM][$BF_4$] systems, while very little work has been done on pure PVDF with [BMIM][$BF_4$]. Although, PVDF-based composites incorporating [BMIM][$BF_4$] IL have been explored in previous studies, but there is still scope to understand how IL incorporation influences the mechanical and thermal behaviour of the PVDF matrix, particularly when both aspects are examined together.

To fill this gap, in the present work, PVDF/[BMIM][$BF_4$] films have been prepared using the solution casting method. The solution casting technique was selected for the preparation of PVDF/[BMIM][$BF_4$] composite films because it allows the IL to be incorporated into the polymer matrix through solution-based mixing. This approach facilitates the preparation of films with different IL concentrations under comparable processing conditions, making it suitable for examining the influence of IL loading on the properties of PVDF. Moreover, the formation of continuous and flexible films makes this technique appropriate for evaluating tensile properties as well as thermal behaviour.

Here, more focus is given to mechanical and thermal properties to understand how adding [BMIM][$BF_4$] changes the strength, flexibility, and thermal stability of PVDF. Along with this, the study also explores the structural behaviour of the solution cast films. This helps in establishing a clear relationship between composition and material properties for practical applications. This work is the initial step to improve the thermal and mechanical properties of PVDF/[BMIM][$BF_4$] which will serve as basis for synthesizing a tricomposite with a ceramic to achieve better piezoelectric performance for energy harvesting devices.

## 2. MATERIALS AND METHODS

### 2.1. Materials

Poly(vinylidene fluoride) (PVDF) with an average molecular weight of 1,80,000 g $mol^{-1}$ was purchased from Sigma-Aldrich, Darmstadt, Germany. N,N-Dimethylformamide (DMF) was obtained from Himedia, Wagle Industrial Estate, Thane (WEST), Maharashtra. The ionic liquid, 1-butyl-3-methylimidazolium tetrafluoroborate ([BMIM][$BF_4$]), (MW=226.03) (>98.0%) (CAS RN: 174501-65-6) was purchased from Tokyo Chemical Industry Co., Ltd. Japan. All chemicals were used as received without any further purification.

### 2.2. Preparation of PVDF/[BMIM][$BF_4$]Films

A 20 wt.% of PVDF was first dissolved in DMF under continuous stirring at 60 °C with 550 rpm until a clear and homogeneous solution was obtained. After complete dissolution, a different amount of ionic liquid was slowly added to the PVDF solution with continuous magnetic stirring. The mixture was further stirred for 24 hours to ensure uniform mixing of the ionic liquid within the PVDF matrix. The prepared solution was cast onto a clean glass Petri dish using the solution casting method. Prior to deposition, the Petri dish was thoroughly cleaned with acetone to ensure a contaminant-free surface for uniform film formation. The cast solution was then allowed to dry at 60 °C for 24 h to completely evaporate the solvent. After complete drying, the free-standing films were carefully peeled off from the Petri dish. The obtained films thickness were varied from 200 μm to 250 μm. The films thickness were measured from screw guage having least count of 0.01mm. To further enhance the β-phase content of PVDF, the dried films were annealed at 110 °C for 5 h and corona poling was

carried out using grid voltage 2 kV, needle voltage 15 kV for 45 minutes at 80°C. The corona poling parameters were taken from the available literature[32]. The concentration of the ionic liquid in the PVDF matrix was varied as 3 wt.%, 6 wt.%, 9 wt.%, 12 wt.% and 15 wt.% and named as PVDF, PVDF-IL-3, PVDF-IL-6, PVDF-IL-9, PVDF-IL-12, and PVDF-IL-15 respectively. The overall preparation procedure of the PVDF/ionic liquid solution cast films is schematically illustrated in Figure **1**.

### 2.3. Characterization Techniques

Scanning Electron Microscopy (SEM) JEOL JSM-6390LV was used to observe the surface morphology of solution cast films. X-ray Diffraction (XRD) with Model no. Bruker D8 Advance diffractometer was used to observe the crystal size and crystallinity of films at room temperature using Cu-Kα radiation (λ = 1.54 Å) at 40 kV and 15 mA. The scan range was 0° to 90° with 0.001° step size. Fourier Transformed Infrared Spectroscopy (FTIR) with Model no. Bruker alpha spectrophotometer was used in the range of 600–4000 $cm^{-1}$ to analyze the α, β phases and to calculate the beta fraction of solution cast films. The electroactive phase fraction (F(EA)) was calculated with the help of FTIR absorption data by using equation 1. The β phase fraction (F(β)) and γ phase fraction (F(γ )) were calculated with the help of FTIR absorption data by using Eq. 2 & Eq. 3

$$F(EA) = \frac{A\beta}{\frac{K\beta}{K\alpha} \times A\alpha + A\beta} \quad (1)$$

$$F(\beta) = F_{EA}\left[\frac{A_{\beta\prime}}{A_{\beta\prime}+A_{\gamma\prime}}\right] \times 100\% \quad (2)$$

$$F(\gamma) = F_{EA}\left[\frac{A_{\gamma\prime}}{A_{\beta\prime}+A_{\gamma\prime}}\right] \times 100\% \quad (3)$$

Where $A_\alpha$ represent absorbance at 763 $cm^{-1}$ and $A_\beta$ absorbance at 840 $cm^{-1}$. $K_\alpha$ the absorption coefficients are 6.1 × 104 $cm^2$ $mol^{-1}$ and $K_\beta$ absorption coefficients are 7.7 × 104 $cm^2$ $mol^{-1}$. Here, $A_{\beta\prime}$ and $A_{\gamma\prime}$ denote the absorbance intensities measured at 1234 $cm^{-1}$ and 1275 $cm^{-1}$, which are associated with the characteristic absorption bands of the β and γ phases, respectively. The Mechanical tensile tests were done using a Universal Testing Machine (UTM,Z010(Static)) on ASTM D882. The size of the films were taken as 50 mm × 10 mm and tested under a 5 N load cell at a 5 mm $min^{-1}$ speed. The Thermo gravimetric analysis (TGA) analysis were carried out using STA hitachi 7000 machine with the heating rate of 10°C/minutes in the presence of Nitrogen ($N_2$) gas.

## 3. RESULTS

### 3.1. FTIR

The crystalline phases of solution –cast films were identified by using FTIR techniques. The corresponding data of PVDF and PVDF-IL films are shown in Figure **2**. The crystal phases of PVDF from reported literature [33], the band at 763 and 872 $cm^{-1}$ can be attributed to non polar -α phase while the bands 840, 1172 , and 1401 $cm^{-1}$ can be assigned to polar form of PVDF with all trans conformation (β phase). The 833 $cm^{-1}$ and

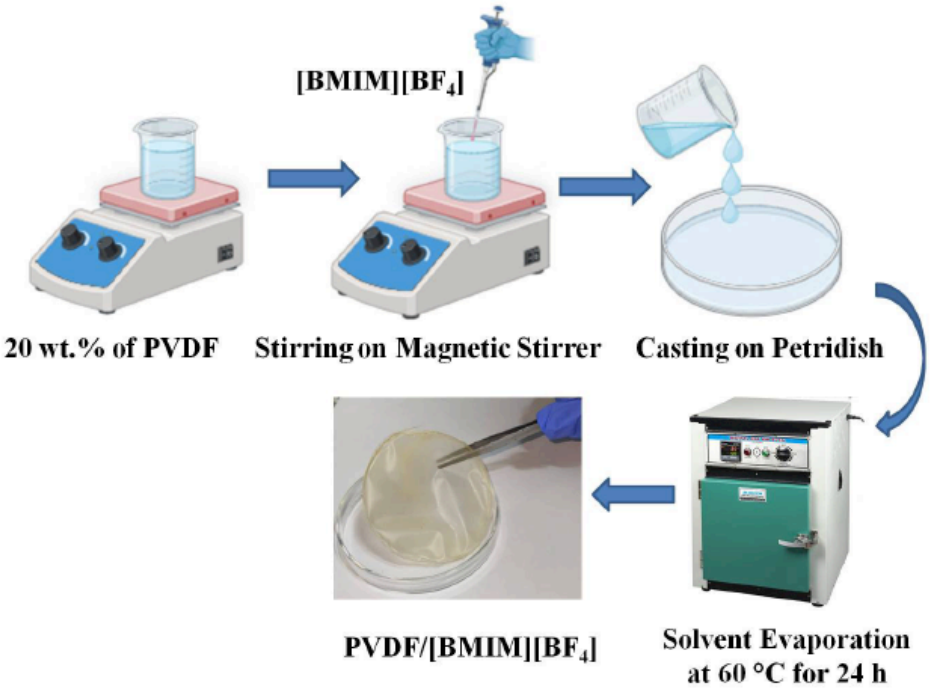



**Figure 1:** Schematic presentation of the fabrication process for PVDF/[BMIM][$BF_4$] films.

1234 $cm^{-1}$ peaks are related to γ-phase showing the γ polar phase was also present in PVDF samples. Therefore, the broad peak seen around 831–840 $cm^{-1}$ is sum of β and γ phase [15]. The F(EA) was calculated by using equation 1 as shown **in** Figure **3a** indicating that the β+γ phase fraction or electroactive phase fraction (F(EA)) of pure PVDF is 53.8% and increases upon the addition of IL increases. The PVDF-IL-12 increases the F(EA) of PVDF from 53.8% to 86.6%. As shown in Figure **3b**, the β-phase fraction increases from 31% in pure PVDF to 54.3% upon the addition of 12 wt% IL (PVDF-IL-12). A similar trend is observed for the γ-phase, whose fraction rises from 13.5% to ~ 32.2%, as presented in Figure **3b**. However, a further increase in IL content to 15 wt% results in a reduction in both phase fractions, with the β- and γ-phase contents decreasing to 42.9% and 21.7%, respectively. These results indicate that PVDF-IL-12 provides a more favourable IL concentration for promoting the formation of both electroactive phases. This confirms that IL addition effectively increase the polar phase of PVDF, which is beneficial for improving the piezoelectric performance of PVDF.

### 3.2. XRD

The XRD measurements were carried out to qualitatively determine the crystal phases present in PVDF and PVDF-IL-12 films. The Figure **4** shows, the samples have a strong peak at 2θ=20.26°, which mainly corresponds to the diffraction peak of the β (200)/(110) planes [33, 34]. The α and β diffraction peak of PVDF are matched with the JCPDS (Joint Committee on Powder Diffraction Standards) database card no. 42-1650, and 38-1638 respectively [35]. The variation in peak intensities in both samples can be attributed to the increase in orientation of the crystals. IL enhanced crystal intensity at 20.26° indicates a higher degree of microcrystal orientation induced by IL. A peak at 2θ = 18.6° is observed in the PVDF film corresponds to the diffraction peak of the α (020) planes. With the increase in IL concentration at

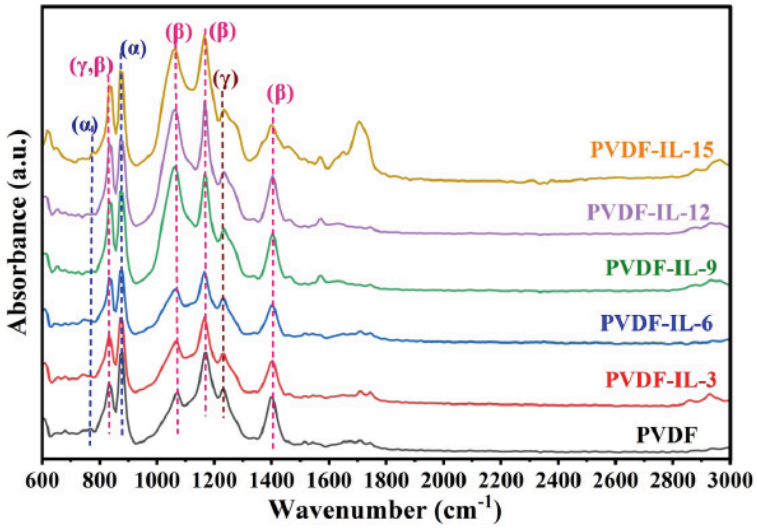



**Figure 2:** FTIR Spectra of (**a**) PVDF, (**b**) PVDF-IL-3, (**c**) PVDF-IL-6, (**d**) PVDF-IL-9, (**e**) PVDF-IL-12 and (**f**) PVDF-IL-15.

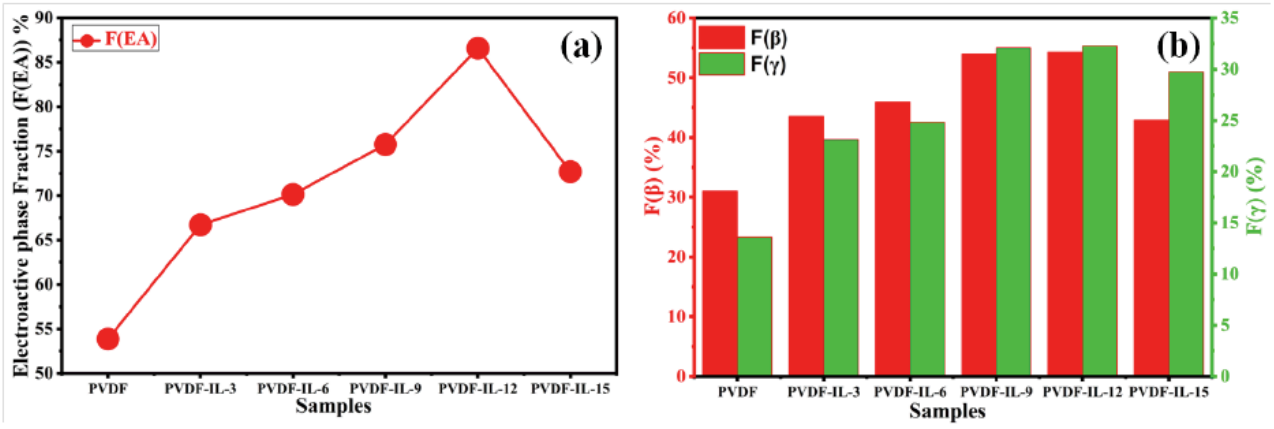



**Figure 3:** Phase content fraction of PVDF and PVDF –IL with different concentration (**a**) electroactive phase fraction (FEA) and (**b**) Beta and Gamma phase fraction.

PVDF-IL-12 as shown in Figure **4** the α phase peak decreases. Furthermore, the reflection observed at ~36–37°, assigned to the β-phase (020)/(101) planes, provides additional support for the development of β-phase crystalline ordering. This peak found to be similar to the available literature[20]. The relative prominence of the β-phase-associated reflections, together with the reduced contribution of the characteristic α-phase reflection, indicates that the IL influences the crystallization behaviour of the PVDF matrix and promotes the formation of its electroactive phase. This transformation can be attributed to interactions between the IL and the polar $–CH_2–$ and $–CF_2–$ groups of PVDF, which may influence chain arrangement and promoting the transformation of the α phase into the all-trans β phase [15]. However, since some diffraction reflections of the α- and β-phases overlap, the XRD results are interpreted alongside FTIR analysis to obtain a more reliable assessment of the phase transformation.

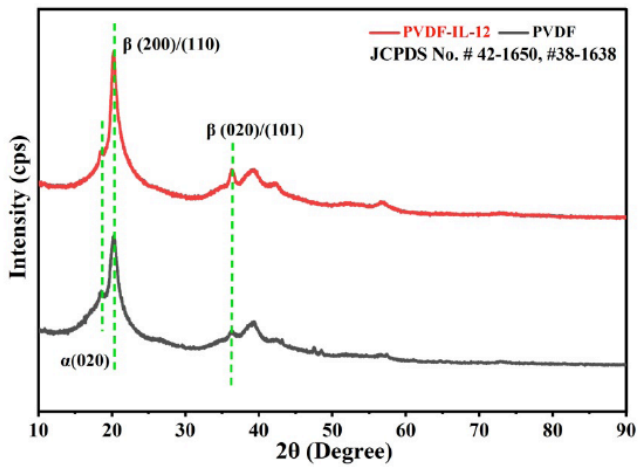



**Figure 4:** X-ray diffraction pattern of PVDF and PVDF-IL-12.

### 3.3. SEM

The SEM images of PVDF-IL composites with different IL concentrations are shown in Figure **5**. It can be seen that the PVDF film without IL exhibits a relatively smooth and void-free surface. At PVDF-IL-3 the surface morphology of PVDF changes and the voids begin to form between the spherical crystals. However, increasing the IL concentration PVDF-IL-6 and PVDF-IL-9 the morphology changes and surface become rough. Also the formation of tightly packed particles like structure observed which indicating the changes in microstructure of PVDF take place. Further, at PVDF-IL-12 and PVDF-IL-15, the surface become smooth as compare to PVDF-IL-9 , which indicating the IL well disperse in PVDF. This is due to the reason since the imidazole cation in the ionic liquid carries a positive charge and the $–CF_2–$ group in PVDF is highly electronegative, they interact strongly with each other. Because of these electrostatic interactions, both materials mix well and become compatible in the molten state [36]. The IL mostly presents in the amorphous regions of PVDF and try to accumulate at the interface between crystalline and amorphous phases. Because of this, the surface morphology shows that IL evaporation leaves behind more uniform and finer dispersion in the material [37].

### 3.4. Mechanical Strength

The mechanical properties of the solution cast PVDF and PVDF-IL film were understood based on their tensile strength and Fracture point (elongation at fracture), as shown in Figure **6**. The result shows that the tensile strength of solution cast PVDF Film reached to its peak at PVDF-IL-12, resulting in 47.85% improved in tensile strength from 14 MPa to 20.7 MPa. The PVDF tensile strength was found similar to that of

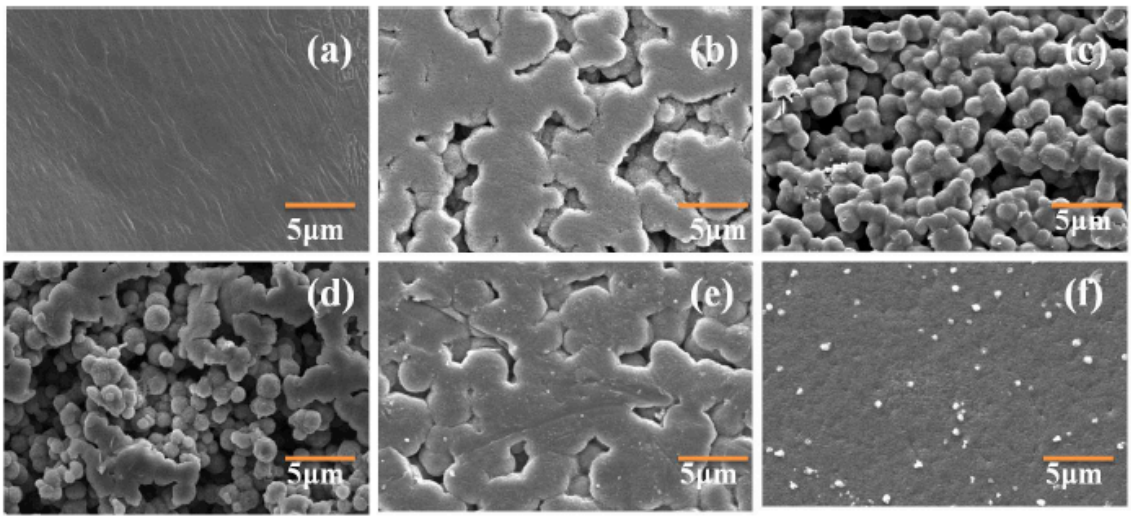



**Figure 5:** SEM images of (**a**) PVDF, (**b**) PVDF-IL-3, (**c**) PVDF-IL-6, (**d**) PVDF-IL-9, (**e**) PVDF-IL-12 and (**f**) PVDF-IL-15.

reported literature [38]. This improvement may be due to stronger interactions between the PVDF chains and IL. Along with the increase in tensile strength, the elongation at fracture also showed a improvement, increasing from 75.07% to 203.1%, indicating enhanced flexibility of the PVDF-IL-12 film. The simultaneous improvement in these two properties shows that the incorporation of an IL enhances both the load-bearing capability and deformability of the PVDF matrix.

This improvement can be associated with the interaction of [BMIM][$BF_4$] ions with the polar groups of PVDF, particularly –$CH_2$– and –$CF_2$– groups. These interactions may modify the intermolecular forces and arrangement of polymer chains, resulting in a more favourable distribution of stress during mechanical deformation [20]. At PVDF-IL-12, the IL may also facilitate polymer-chain mobility, allowing the chains to undergo greater deformation before fracture without compromising the strength of the material. Thus, the combined effect of modified chain interactions and enhanced flexibility may improved mechanical performance of PVDF-IL-12.

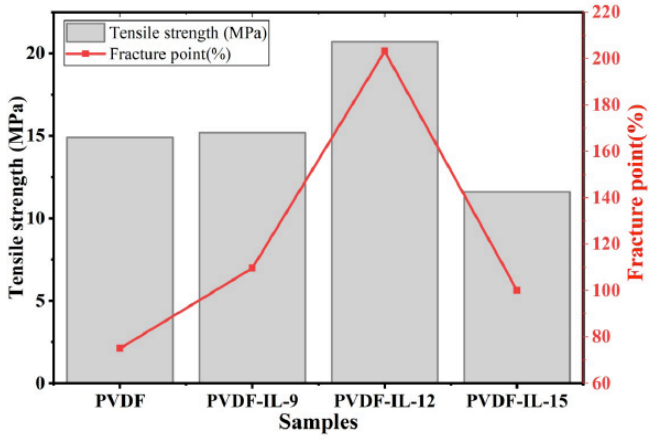



**Figure 6:** Tensile strength and Fracture point of solution cast PVDF and PVDF/IL films.

However, after PVDF-IL-12 sample, both the tensile strength and elongation at fracture begin to decrease. This reduction can be attributed to the excess IL content, which leads to plasticization and phase separation, thereby weakening the intermolecular interactions among PVDF chains and reducing the overall mechanical strength of the PVDF films. The films fabricated in this study demonstrate higher tensile strength as well as enhanced elongation at fracture in comparison to previously reported [BMIM][$BF_4$] incorporated into PVDF membranes. In that study, the PVDF/[BMIM][$BF_4$] membrenes were fabricated via non-solvent thermally induced phase separation (N-TIPS) , resulting in tensile strength upto 7.43 MPa and elongation at break upto 134.9% [20]. In another study, a different organic ILs were incorporated into PVDF foam, fabricated by foam machine in which a 0.5 wt.% of [BMIM][$BF_4$] / PVDF foam showed a tensile strength of 0.27 MPa [18]. Therefore, the results showed the balance in mechanical properties, where both tensile strength and elongation at fracture improve upto PVDF-IL-12.

### 3.5. TGA

Thermogravimetric analysis (TGA) was carried out to understand the incorporation of IL into PVDF effects the thermal stability of the PVDF-IL film as shown in Figure **7**. Figure **7a** shows the mass loss (%) with respect to temperature (°C) of PVDF and PVDF-IL solution cast films. The TGA curves of all films show good thermal stability up to 320 °C. No weight loss below 200 °C in the solution cast films indicates that the samples are free from any solvent or moisture. This observation is consistent with the hydrophobic nature of the fluoropolymer and the moisture stability of imidazolium-based ionic liquids[30]. Based on earlier studies, the thermal degradation temperature ($T_d$) of PVDF is ~ 470 °C, whereas for [BMIM][$BF_4$], it lies between 300 °C to 420 °C [39, 40]. The $t_d$ begins and takes place in two stages of mass loss, as also reported in previous studies [41, 42]. PVDF exhibits thermal stability, with the $t_d$ occurring at ~ 430 °C, followed by a mass loss between 450 and 520 °C, indicating the decomposition of the polymer backbone[28]. While the PVDF-IL solution cast films show an decrease in $t_d$ at ~ 370 °C, which can be attributed to the lower thermal stability of the incorporated IL. This shift towards a lower temperature can be due to the lower thermal decomposition temperature of the incorporated IL. The presence of [BMIM][$BF_4$] introduces additional thermally decomposable components into the PVDF matrix, thereby modifying its overall degradation behaviour [30].

The major weight loss for PVDF-IL solution cast films occur in the range of 370–420 °C, indicating that the presence of IL accelerates the degradation process. However, the PVDF-IL-12 film remains stable up to 327 °C, showing that the film can withstand thermal exposure within this temperature range before the onset of major degradation and is suitable for many practical applications. Furthermore, the residue at 700 °C for pure PVDF is found to be 1.23%, indicating almost complete decomposition, whereas PVDF-IL-12 exhibits a 36.2% residue. This difference in residue concentration shows that the incorporation of [BMIM][$BF_4$] changes the decomposition pathway and the nature of the final products formed during thermal degradation. The higher residue may be associated with the formation of non-volatile decomposition products, including possible carbonaceous and inorganic residues originating from the IL-containing

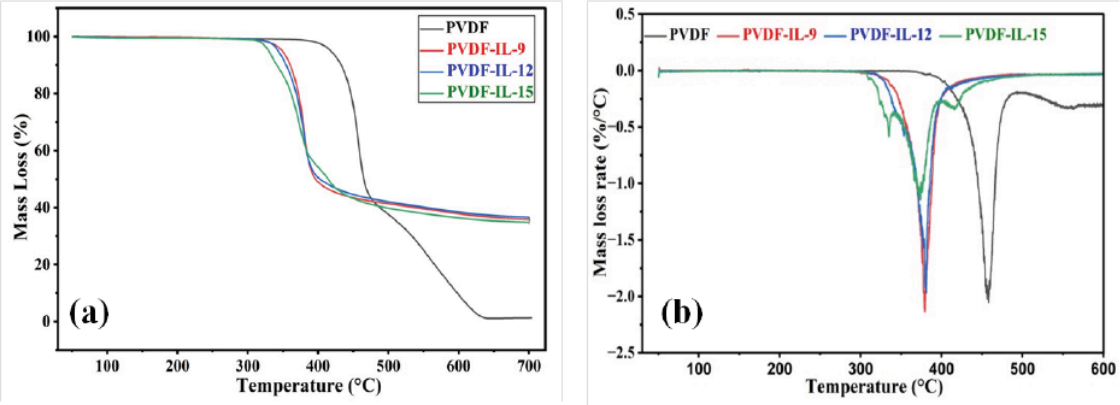



**Figure 7:** (**a**) Mass loss % w.r.t. temperature of PVDF and PVDF-IL with different concentration of IL (TGA) (**b**) first derivative of TGA curve (DTG) w.r.t temperature.

composite [41]. However, the exact chemical composition of the residual material cannot be confirmed through TGA alone and requires further characterization. Therefore, the higher residual mass should not be considered direct evidence of improved thermal stability; rather, it indicates a change in the final decomposition characteristics of the PVDF-IL film.

The DTG curve in Figure **7b** exhibits a sharp degradation peak for each films. The PVDF-IL-9 and PVDF-IL-12 results in a single sharp peak at 379°C, shows that the [BMIM][$BF_4$] incorporated in PVDF matrix. The PVDF-IL-15, there is three peaks in which the degradation peak at 419 °C, corresponds to the thermal decomposition of the PVDF matrix [43]. The appearance of multiple peaks suggests a more complex degradation process, which may involve different decomposition stages of the polymer and incorporated IL [41, 42].

The observed shift in degradation temperature confirms that the incorporation of IL modifies the thermal degradation behaviour of the PVDF matrix. Despite this reduction, the material remains thermally stable upto 327°C temperature range, making it suitable for use in sensors, actuators, energy harvesting/storage, and high-temperature applications.

### 3.6. Comparison of Present Work with Reported Data

A comparison of present work with reported data has been shown in Table **1**. Previous studies focused on PVDF-HFP/[BMIM][$BF_4$], where thermal stability has been reported but mechanical properties are missing by solution casting method. Limited studies are available on pure PVDF/[BMIM][$BF_4$], and a combined analysis of thermal and mechanical properties is still lacking. In this work, pure PVDF/[BMIM][$BF_4$] solution cast films are prepared using the solution casting method and both thermal and mechanical properties are studied together. The results show thermal stability up to 327 °C along with elongation at break up to 203.1%, making the material suitable for practical applications.

## CONCLUSION AND FUTURE SCOPE

In this study, PVDF-IL films were successfully fabricated using the solution casting method. The effect

**Table 1: Comparison of Mechanical and Thermal Data of PVDF/[BMIM][$BF_4$] Solution Cast Film by Reported Data**

| Samples | Fabrication Techniques | Composition of [BMIM][$BF_4$] of wt.% of PVDF | β Fraction | Tensile Strength (MPa) | Elongation at Break | Thermal Stability | References |
|---|---|---|---|---|---|---|---|
| PVDF | Solution casting | - | 53.8% | 14.9 | 75.07% | 420°C | [38] |
| PVDF/[BMIM][$BF_4$] | Foaming | - | 85% | 0.27 | 20% | - | [18] |
| PVDF HFP/[BMIM][$BF_4$] | Solution casting | 40 wt.% % | - | | - | 300°C | [30] |
| PVDF/[BMIM][$BF_4$] | N-TIPS | %(only one come) | - | 7.43 | 134.9% | - | [20] |
| PVDF-HFP/[BMIM][$BF_4$] | Solution casting | 90 wt.% | - | | - | 320°C | [28] |
| PVDF-HFP/[BMIM][$BF_4$] | Solution casting | 4 wt.% | - | | - | 370°C | [31] |
| PVDF/[BMIM][$BF_4$] | Spin Coating | 6 wt.% | 43.8% | 17.6 | 157.2% | - | [44] |
| **PVDF/[BMIM][$BF_4$]** | **Solution Casting** | **12 wt.%** | **86.6%** | **20.7** | **203.1%** | **327°C** | **Present work** |

of IL concentration on structural, morphological, mechanical, and thermal were investigated. The results showed that the incorporation of IL tailor the overall performance of PVDF films. The FTIR and XRD analysis showed a enhancement in β-phase with the addition of ILs, with the maximum $F_\beta$ ~ 86.6% observed at PVDF-IL-12. The mechanical analysis showed that the tensile strength and elongation at break of PVDF-IL-12 also increases, showing improved flexibility and strength due to enhanced intermolecular interactions. The thermal analysis showed that the PVDF- IL-12 reduced the degradation temperature of PVDF. Therefore, among all PVDF-IL solution cast films, PVDF-IL-12 exhibited the enhanced β-phase, improved mechanical and acceptable thermal stability. The PVDF/[BMIM][$BF_4$] was fabricated to improve the mechanical and thermal properties of PVDF, where the incorporation of [BMIM][$BF_4$] increases the flexibility of PVDF which is important parameter for wearable energy harvesting application. In the next step, a tricomposite using PVDF/[BMIM][$BF_4$] incorporating ceramic material will be synthesized to enhance the thermal performance and piezoelectric properties for energy harvesting applications in wearables.

## ACKNOWLEGMENT

The authors thank to the Kurukshetra University, Kurukshetra (KUK), for their financial support through the University Research Scholarship. The authors also thank to CAMR (Centre For Advanced Material Research) under RUSA 2.0, Department of Physics, KUK for providing access to XRD and Department of Chemistry, KUK for FTIR characterization facilities. The authors acknowledge National Institute Of Technology, Kurukshetra for SEM characterization.

## AUTHOR CONTRIBUTIONS

**Kavita Rani:** Conceptulization, Methodology, Validation, Investigation, Writing Original Draft.

**Anurekha Sharma:** Supervision, Writing-Reviewing and Editing.

**Yashashchandra Dwivedi:** Supervision, Writing-Reviewing and Editing.

## COMPETING INTERESTS

The authors have no relevant financial or non-financial interests to disclose.

## DATA AVAILABILITY STATEMENT

All data generated or analyzed during this study are included in the main body of the article. No additional datasets were created or made available.

## REFERENCES

[1] F. P. Materials. Properties and applications of flexible poly(vinylidene fluoride)-based piezoelectric materials. 2021; p. 1-21.

[2] Ruan L, Yao X, Chang Y, Zhou L, Qin G, Zhang X. Properties and applications of the β phase poly(vinylidene fluoride). Polymers (Basel). 2018; 10(3): 1-27. https://doi.org/10.3390/polym10030228

[3] Alam MM, Crispin X. The past, present, and future of piezoelectric fluoropolymers: Towards efficient and robust wearable nanogenerators. Nano Research Energy. 2023. https://doi.org/10.26599/NRE.2023.9120076

[4] Pickford T, Gu X, Heeley EL, Wan C. Effects of an ionic liquid and processing conditions on the β-polymorph crystal formation in poly(vinylidene fluoride). Cryst Eng Comm. 2019; 21(36): 5418-5428. https://doi.org/10.1039/C9CE01051C

[5] Bhadwal N, Ben Mrad R, Behdinan K. Review of piezoelectric properties and power output of PVDF and copolymer-based piezoelectric nanogenerators. Nanomaterials. 2023; 13(24): 3170. https://doi.org/10.3390/nano13243170

[6] Chen B, *et al*. Flexible piezoelectrics: Integration of sensing, actuating and energy harvesting. Nature Reviews Electrical Engineering. 2025. https://doi.org/10.1038/s41528-025-00432-5

[7] Jurczuk K, Galeski A, Mackey M, Hiltner A, Baer E. Orientation of PVDF α and γ crystals in nanolayered films. J Polym Res. 2015; 22: 1289-1297. https://doi.org/10.1007/s00396-015-3542-7

[8] Martins P, Lopes AC, Lanceros-Méndez S. Electroactive phases of poly(vinylidene fluoride): Determination, processing and applications. Prog Polym Sci. 2014; 39(4): 683-706. https://doi.org/10.1016/j.progpolymsci.2013.07.006

[9] Li H, Liang J, Zheng R, Zhu H, Zhao W, Li Y. Influence of β-phase content on the stretching-induced α-β phase transition of highly oriented poly(vinylidene fluoride) ultrathin films. 2025. https://doi.org/10.1007/s10118-025-3358-y

[10] Gomes J, Nunes JS, Sencadas V. Influence of the β-phase content and degree of crystallinity on the piezo- and ferroelectric properties of poly(vinylidene fluoride). Smart Mater Struct. 2010; 19(6): 065010. https://doi.org/10.1088/0964-1726/19/6/065010

[11] Gee S, Johnson B, Smith AL. Optimizing electrospinning parameters for piezoelectric PVDF nanofiber membranes. J Membr Sci. 2018; 563: 804-812. https://doi.org/10.1016/j.memsci.2018.06.050

[12] Park JH, Kurra N, Almadhoun MN, Odeh IN, Alshareef HN. Ferroelectric properties of poly(vinylidene fluoride). J Mater Chem C. 2015; 3: 2366-2370. https://doi.org/10.1039/C4TC02079K

[13] Ghafari E, Jiang X, Lu N. Surface morphology and beta-phase formation of single polyvinylidene fluoride (PVDF) composite nanofibers. 2017. https://doi.org/10.1007/s42114-017-0016-z

[14] Mahdavi Varposhti A, Yousefzadeh M, Kowsari E, Latifi M. Enhancement of β-phase crystalline structure and piezoelectric properties of flexible PVDF/ionic liquid surfactant composite nanofibers for potential application in sensing and self-powering. Macromol Mater Eng. 2020; 305(3): 1900796. https://doi.org/10.1002/mame.201900796

[15] Zhou R, *et al*. Effects of ionic liquid content on the electrical properties of PVDF films by fused deposition modeling. Materials (Basel). 2024; 17(1): 9. https://doi.org/10.3390/ma17010009

[16] Liu X, Shang Y, Zhang J, Zhang C. Ionic liquid-assisted 3D printing of self-polarized β-PVDF for flexible piezoelectric energy harvesting. ACS Appl Mater Interfaces. 2021; 13(12): 14334-14341. https://doi.org/10.1021/acsami.1c03226

[17] Ye Z, Yi J, Zhang Y, Xiong C. Significantly enhanced piezoelectricity of poly(vinylidene fluoride) via orienting nanobound state ions. Adv Mater Technol. 2025; 10(7): 1-8. https://doi.org/10.1002/admt.202401447

[18] Zhao Y, Liu G, Guo M, Li G, Liao X. Tunable polar phase content in lightweight poly(vinylidene fluoride) foam for piezoelectric applications. Polymer. 2025; 334: 128758. https://doi.org/10.1016/j.polymer.2025.128758

[19] He L, Sun J, Wang X, Wang C, Song R, Hao Y. Facile and effective promotion of β crystalline phase in poly(vinylidene fluoride) via the incorporation of imidazolium ionic liquids. Polym Int. 2013; 62(4): 638-646. https://doi.org/10.1002/pi.4339

[20] He T, *et al*. Poly(vinylidene fluoride) (PVDF) membrane fabrication with an ionic liquid via non-solvent thermally induced phase separation (N-TIPS). Appl Water Sci. 2022; 12(3): 1-11. https://doi.org/10.1007/s13201-021-01499-x

[21] Kadyrova ZR, Eminov AA, Usmonov HL, Khonimkulov ZA, Tairov SS. Physicochemical study of hematite rock from the Kyzyltash deposit for the production of ceramic pigments. 2026; p. 1-5. https://doi.org/10.31875/2410-4701.2026.13.01

[22] Mejri R, Dias JC, Hentati SB, Martins MS, Costa CM, Lanceros-Méndez S. Effect of anion type in the performance of ionic liquid/poly(vinylidene fluoride) electromechanical actuators. J Non Cryst Solids. 2016; 453: 8-15. https://doi.org/10.1016/j.jnoncrysol.2016.09.014

[23] Xing C, You J, Li Y, Li J. Nanostructured poly(vinylidene fluoride)/ionic liquid composites: Formation of organic conductive nanodomains in polymer matrix. J Phys Chem C. 2015. https://doi.org/10.1021/acs.jpcc.5b05349

[24] Botelho G, *et al*. High performance electromechanical actuators based on ionic liquid/poly(vinylidene fluoride). Polym Test. 2015; 48: 199-205. https://doi.org/10.1016/j.polymertesting.2015.10.012

[25] Shilin AD. The effect of sonication on the dielectric properties of ceramics. 2026; p. 11-19. https://doi.org/10.31875/2410-4701.2026.13.03

[26] Rinkevich AB, Perov DV, Kuznetsov EA, Stenina MS. Magnetic and high-frequency dielectric properties of stuffed pyrochlore Er2TiO5. 2026; p. 20-27. https://doi.org/10.31875/2410-4701.2026.13.04

[27] Razzaq H, *et al*. Hybrid ionogel membrane of PVDF incorporating ionic liquid-reduced graphene oxide for the removal of heavy metal ions from synthetic water. Mater Sci Eng B. 2023; 296: 116680. https://doi.org/10.1016/j.mseb.2023.116680

[28] Bf BK. Thermal stability, complexing behavior, and ionic transport of polymeric gel membranes based on polymer PVdF-HFP and ionic liquid, [BMIM][BF4]. 2013.

[29] Dias JC, Correia DM, Costa CM, Botelho G, Vilas-Vilela JL. Thermal degradation behavior of ionic liquid/fluorinated polymer composites: Effect of polymer type and ionic liquid anion and cation. Polymer. 2021; 229: 123995. https://doi.org/10.1016/j.polymer.2021.123995

[30] Dzulkipli MZ, *et al*. The influences of 1-butyl-3-methylimidazolium tetrafluoroborate on electrochemical, thermal and structural studies as ionic liquid gel polymer electrolyte. Polymers (Basel). 2021; 13(8): 1277. https://doi.org/10.3390/polym13081277

[31] Yongquan D, Ming W, Lin C, Mingjun L. Preparation, characterization of P(VDF-HFP)/[BMIM]BF4 ionic liquids hybrid membranes and their pervaporation performance for ethyl acetate recovery from water. Desalination. 2012; 295: 53-60. https://doi.org/10.1016/j.desal.2012.03.018

[32] Mahadeva SK, Berring J, Walus K, Stoeber B. Effect of poling time and grid voltage on phase transition and piezoelectricity of poly(vinylidene fluoride) thin films using corona poling. 2013; 46. https://doi.org/10.1088/0022-3727/46/28/285305

[33] Roni NP, *et al*. Optimizing β-phase content in PVDF membranes via modification of dope solution with citric acid/nano-TiO2 using nonsolvent-induced phase separation method. 2025. https://doi.org/10.3390/polym17040481

[34] Shen Y, Li Z, Liu Y, Wang JT. Impact of hot rolling on the structure and electrical properties of solution cast PVDF films and its optimization in sensors. 2025; 514. https://doi.org/10.1016/j.cej.2025.163361

[35] Nikoli Z, Pele A, Aleksi O, Pavlovi VP, Djokovi V, Doj R. Structural and electrical properties of ferroelectric poly(vinylidene fluoride) and mechanically activated ZnO nanoparticle composite films. Phys Scr. 2018; 93. https://doi.org/10.1088/1402-4896/aad749

[36] Xu P, Fu W, Luo X, Ding Y. Enhanced dc conductivity and conductivity relaxation in PVDF/ionic liquid composites. Mater Lett. 2017; 206: 60-63. https://doi.org/10.1016/j.matlet.2017.06.104

[37] Wang P, Pan Z, Wang M, Huang S, Liu J, Zhai J. Polypyrrole random-coil induced permittivity from negative to positive in all-organic composite films. J Mater. 2019; 1-7.

[38] Chan MK, Tan SJ, Yeow ATH, Ng SC, Lau WJ. Zeolite-based poly(vinylidene fluoride) ultrafiltration membrane: Characterization and molecular weight cut-off estimation with support vector regression modelling. 2024. https://doi.org/10.3390/membranes14040091

[39] Ervin MH, Levine LB, Nichols BM, Parker TC, Ervin MH. Thermal processing for graphene oxide supercapacitor electrode reduction and wetting. J Appl Electrochem. 2016; 46(10): 1075-1084. https://doi.org/10.1007/s10800-016-0991-8

[40] Park YS, Ha C, Kang SW. Highly permeable ionic liquid 1-butyl-3-methylimidazolium tetrafluoroborate-based membrane. RSC Adv. 2017; 7: 33568-33571. https://doi.org/10.1039/C7RA04797E

[41] Caparros SFMCMCC. Effect of filler size and concentration on the structure and properties of poly(vinylidene fluoride)/BaTiO3 nanocomposites. J Mater Sci. 2012; 47: 1378-1388. https://doi.org/10.1007/s10853-011-5916-7

[42] Silva DJ, Contreras MM, Nascimento CR, Ferreira M. Kinetics of thermal degradation and lifetime study of poly(vinylidene fluoride) (PVDF) subjected to bioethanol fuel accelerated aging. Heliyon. 2020; 6. https://doi.org/10.1016/j.heliyon.2020.e04573

[43] Behrens M, Cross S, Akasaka H, Ohtake N. Pyrolysis of cellulose mixed with ionic liquids 1-butyl-3-methylimidazolium bis(trifluoromethylsulfonyl)imide [BMIM][TFSI], 1-butyl-3-methylimidazolium tetrafluoroborate [BMIM][BF4], and 1-butyl-2,3-dimethylimidazolium tetrafluoroborate [BMMIM][BF4]. Biomass Bioenergy. 2019; 122: 290-297. https://doi.org/10.1016/j.biombioe.2019.01.029

[44] Rani K, Sharma A, Dwivedi Y. Spin coated polyvinylidene difluoride/ionic liquid nanocomposite thin films with enhanced dielectric and piezoelectric properties. J Polymer Compos. 2026; 14(Special Issue 1).

https://doi.org/10.31875/2410-4701.2026.13.11

© 2026 Rani *et al.*
This is an open-access article licensed under the terms of the Creative Commons Attribution License (http://creativecommons.org/licenses/by/4.0/), which permits unrestricted use, distribution, and reproduction in any medium, provided the work is properly cited.